

Supporting Information Available for

Volcano-shape glycerol oxidation activity of palladium-decorated gold nanoparticles

*Zhun Zhao, Joni Arentz, Lori A. Pretzer, Pongsak Limpornpipat, James M. Clomburg, Ramon Gonzalez, Neil Schweitzer, Tianpin Wu, Jeffrey T. Miller and Michael S. Wong**

Detailed Au and Pd NP synthesis method:

For Au NPs, 5 wt% HAuCl₄ solution (0.126 M) was prepared by dissolving 5 g of HAuCl₄·3H₂O (>99%, Sigma-Aldrich) in 100 mL of deionized (DI) water (>18 MΩ.cm, Barnstead NANOpure Diamond). Separate solutions of 1 wt% sodium citrate, 1 wt% tannic acid (TA), and 25 mM potassium carbonate (K₂CO₃) were prepared by dissolving 0.2 g of sodium citrate dihydrate (>99.5%, Fisher), 0.2 g of tannic acid (>99.5%, Sigma-Aldrich) and 0.049 g of potassium carbonate (>99.5%, Sigma-Aldrich) into 20 mL of H₂O, respectively. A gold salt precursor solution was prepared by adding 200 μL of 5 wt% HAuCl₄ solution into 79.8 mL of H₂O and heating to 60 °C in a water bath with moderate stirring. The reducing agent was prepared by adding 5 mL of TA solution, 5 mL of K₂CO₃ solution, and 4 mL of citrate solution into 6 mL of DI water and also heating to 60 °C. The two solutions were kept at 60 °C for at least 2 min before combining and mixing. Au NP formation occurred instantaneously after adding the reducing agent to the diluted gold solution, evidenced by a color change from clear to ruby-red. The resulting solution was heated to a boil, left boiling for 2 min, and removed from the heat source. The sol was then diluted with H₂O to 100 mL, and left to cool overnight to ambient temperature before being refrigerated. The Au NP concentration was calculated to be 1.07×10¹⁴ NP/mL (= 49.7 mg Au/L), assuming complete reduction of the Au salt and a 7-shell magic cluster model of a 4-nm Au particle.¹⁻⁵

The Pd NPs were prepared in the same manner, except that the Au salt precursor solution was replaced with a palladium salt solution (12 mL of H₂PdCl₄ solution (2.49 mM) diluted in 68 mL of H₂O) and the

boiling time was increased to 25 min. The H_2PdCl_4 solution was prepared by dissolving 42.2 mg $PdCl_2$ (99.99%, Sigma-Aldrich) in 95 mL DI water containing 500 μ L HCl solution (1 M, Fisher Scientific). The resulting sol was dark coffee-brown in color, with a calculated particle concentration of 1.27×10^{14} NP/mL (= 31.8 mg Pd/L) assuming complete reduction of the Pd salt and a 7-shell magic cluster model of a 4-nm Pd particle.¹⁻⁵

Determination of mass transfer effects:

The gas-liquid, liquid-solid, intraparticle diffusion resistances ($1/k_{gl}a_{gl}$, $1/k_{ls}a_s$ and $1/k_i a_i$) and surface reaction resistance ($1/k_{aNP}$) can be correlated in the relation:

$$1/k_{meas} = C_1 + C_2 \times 1/C_{metal} \dots \dots \dots (1)$$

, where C_1 relates to $1/k_{gl}a_{gl}$ and the slope C_2 relates to $1/k_{ls}a_s$, $1/k_i a_i$ and $1/k_{aNP}$, k_{gl} is the gas-liquid mass transfer coefficient, a_{gl} is the gas-liquid interface specific areas, k_{ls} is the liquid-solid mass transfer coefficient, a_s is the exterior specific surface areas of carbon, k_i is the intraparticle diffusion coefficient, a_i is the interior specific surface areas of carbon, k is the rate constant for surface reaction, and a_{NP} is the specific surface areas of NPs.

The liquid-solid mass transfer coefficient k_{ls} toward a spherical particle could be estimated by the Ranz-Marshall correlation, $Sh = 2 + 0.6 \times Re^{1/2} Sc^{1/3}$. For our catalytic heterogeneous system, the maximum Reynolds number, Re , is calculated to be 1514, and the Schmidt number, Sc , is 243 at 60 °C assuming the carbon particles were well suspended with ideal spherical shapes ($d_p = 125 \mu$ m). This gives a Sh value of 147.7. k_{ls} can be estimated to be 2.27×10^{-3} m/s from $Sh = k_{ls} d_p / D_{gly}$, where D_{gly} (= 1.925×10^{-9} m²/s) is the diffusivity of glycerol in 60 °C water.^{6,7} Catalyst exterior surface area in overall batch reactor liquid volume, a_s was calculated to be 2.24×10^2 m²/m³ based on the density of carbon (0.40 g/mL) and volume of the reactor (107 mL). $1/k_{ls}a_s$ can be then calculated to be 5.46×10^{-3} h.

Intraparticle diffusion resistance can be analyzed by the first-order Thiele modulus Φ from the following equation: $\Phi[1/\tanh(3\Phi)-1/(3\Phi)] = -R_{gly} a^2 / (D_{eff} C_{GLYS})$, where C_{GLYS} is glycerol surface concentration (which is assumed to be equal to the bulk fluid glycerol concentration of 0.1 mol/L), R_{gly} is the observed reaction rate ($= -k_{meas} \times C_{GLYS} = -1.32 \text{ h}^{-1} \times 0.1 \text{ mol/L} \div 3600 \text{ s/h} = -3.67 \times 10^{-5} \text{ mol/L/s}$), and a is the characteristic length ($= d_p/6$ for a sphere, $d_p = 20.8 \mu$ m). D_{eff} of glycerol in typical carbon material is 6.83×10^{-10} m²/s (Demirel et al., *Top. Catal.*, **2007**, *44*, 299). This gives a Φ value of 0.015, much smaller than 1. The effectiveness factor η ($= 1/\Phi \times [1/\tanh(3\Phi)-1/(3\Phi)]$) is then calculated to be ~ 1.00 , indicating the intra-particle diffusion for 60 sc% Pd-on-Au/C catalyst can be neglected for glycerol oxidation. C_1 and C_2 can be calculated from Fig. 2b, where the reciprocal of non-zero k_{meas} was plotted against the reciprocal of the concentration of catalyst charged. At a stirring rate of 1000 rpm, the mass transfer resistances terms were determined to be 0.1577, 5.46×10^{-3} , and 0.5999 ($1/\eta k_{a_s} = 1/(C_{Pd} \times k_{cat}) -$

$1/k_{gl}a_{lg} - 1/k_{ls}a_s)$ h for $1/k_{gl}a_{lg}$, $1/k_{ls}a_s$, $1/k_i a_i$ and $1/k_{aNP}$, respectively. The relative order $1/k_{aNP} > 1/k_{gl}a_{lg} \gg 1/k_{ls}a_s$ indicates that resistance from liquid-solid is negligible, while resistance from surface reaction is dominating and gas-liquid mass transfer resistance should be corrected. To exclude the gas-liquid mass transfer effect, observed rate constant should be corrected from:

$$1/k_{corr} = 1/k_{meas} - 1/k_{gl}a_{lg} \dots \dots \dots (2)$$

For 60 sc% Pd-on-Au/C catalyst, k_{corr} was calculated to be 1.67 h^{-1} , which is 26% higher than the k_{meas} (1.32 h^{-1} , Table. 2). Since mass transfer resistances are independent of the active species on catalyst surface, we performed similar calculations for all the rest catalysts to provide k_{corr} values for more accurate calculation of TOF values.

At 700 rpm stirring rate, the gas-liquid mass transfer resistance (y-intercept) was found much greater than at 1000 rpm while liquid-solid and intraparticle diffusion resistances (slope) were the same as at 1000 rpm (Fig. 2b). At 350 rpm stirring rate, the catalyst powder was found to be agglomerating and precipitating at the bottom of the reactor, in which case the mass transfer equation is no longer applicable.

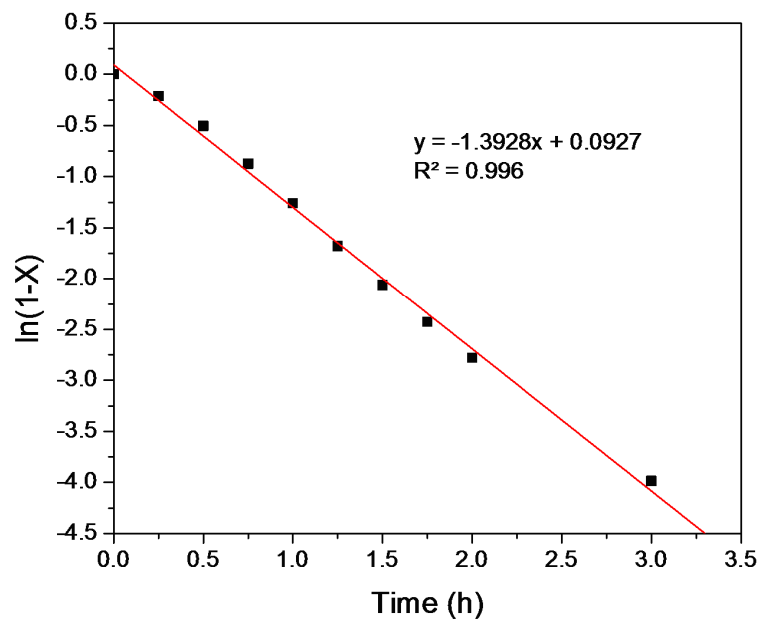


Figure S1. Plot of $\ln(1-x)$ vs. time for 60 sc% Pd-on-Au/C catalyst. Reaction conditions: 0.2 g 60 sc% Pd-on-Au/C, 60 °C, 1000 rpm, 107 mL, 0.1 M glycerol, 0.4 M NaOH, and 120 mL/min O₂ flow.

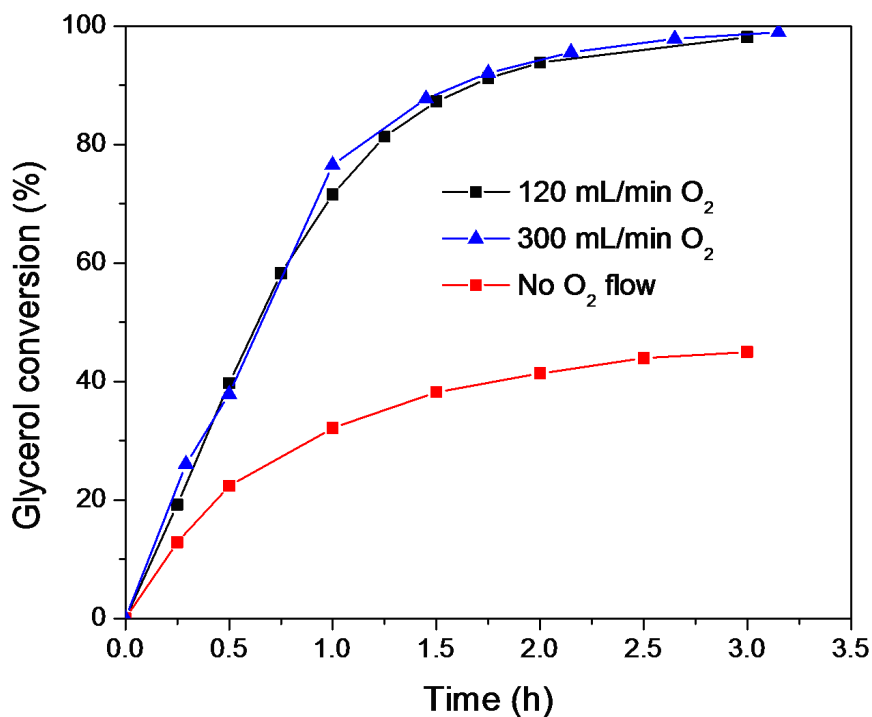


Figure S2. Glycerol conversion-time profiles for glycerol oxidation reaction with O₂ flowing at 120 mL/min, 300 mL/min, and without O₂ flow (1 atm 150 mL headspace O₂ only). Reaction conditions: 0.2 g 60 sc% Pd-on-Au/C, 60 °C, 1000 rpm, 107 mL, 0.1 M glycerol, and 0.4 M NaOH.

Table S1. Comparison of preparation method, metal loading, NP size, TOF, and selectivity to glyceric acid for various catalysts in literature.

Catalyst	Preparation method	Metal loading (wt%)	NP size (nm)	TOF (mol/mol-total-atom/h)	TOF (mol/mol-surface-atom/h) ^g	Selectivity to glyceric acid ^h	Reference
Au/graphite	sol immobilization	1.0	N/A	321.3 ^a	-	78.5% (S ₅₀)	8
Au/C	sol immobilization	1.0	4.0	500 ^b	1438	35.8% (S ₁₀₀)	9
Pd/C	sol immobilization	1.0	5.0	106 ^b	337	74.5% (S _{21.1})	9
AuPd/C	sol immobilization	total: 1.0	5.1	3999 ^b	-	44.1% (S ₁₀₀)	9
Au/C	wet impregnation	1.0	2-10	43 ^c	-	42.5% (S _{34.5})	9
Pd/C	wet impregnation	1.0	2-10	50 ^c	-	61.6% (S _{39.8})	9
AuPd/C	wet impregnation	Au: 2.5, Pd: 2.5	3-8	110 ^c	-	72.5% (S _{87.6})	9
Au/C	sol immobilization	1.0	2-3	1090 ^d	-	64.5% (S ₅₀)	10
Pd/C	sol immobilization	1.0	2-3	1151 ^d	-	80.6% (S ₅₀)	10
AuPd/C	sol immobilization (Au first, Pd next)	total: 1.0 (atomic ratio Au:Pd=1:1)	2-3	1774.5 ^d	-	77.2% (S ₅₀)	10
AuPd/C	sol immobilization (Pd first, Au next)	total: 1.0 (atomic ratio Au:Pd=1:1)	2-3	1765.2 ^d	-	76.5% (S ₅₀)	10
AuPd/C	sol immobilization (Au Pd co-reduction)	total: 1.0 (atomic ratio Au:Pd=1:1)	2-3	1510.0 ^d	-	76.7% (S ₅₀)	10
Au/C	sol immobilization	1.0	N/A	1000 ^e	-	68% (S ₉₀)	11
Pd/C	sol immobilization	1.0	N/A	1000 ^e	-	80% (S ₉₀)	11
AuPd/C	sol immobilization for Au/C, then Pd reduction.	total: 1.0 (atomic ratio Au:Pd=9:1)	N/A	4400 ^e	-	75% (S ₉₀)	11
Au/C	sol immobilization	0.5	5.0	61200 ^f	30527	65% (S ₅₀)	12
Pd/C	commercial	2.9	2.9	3600 ^f	2404	82% (S ₅₀)	12
AuPd/C	reduction of Au onto commercial Pd/C	Pd: 2.9, Au: 0.8	3.2	16560 ^f	-	84% (S ₅₀)	12

^a Calculated after 1 h of reaction. Reaction conditions: 50 °C, 10 mL, 0.3 M glycerol, NaOH: glycerol= 4, glycerol: M= 500, 3 bar O₂.

^b Calculated at 0.5 h reaction, based on the total loading of metals. Reaction conditions: 60 °C, 20 mL, 0.6 M glycerol, NaOH: glycerol= 2, glycerol: M= 2000, 10 bar O₂.

^c Calculated at 0.5 h reaction, based on the total loading of metals. Reaction conditions: 60 °C, 20 mL, 0.6 M glycerol, NaOH: glycerol= 2, glycerol: M= 500, 10 bar O₂.

^d Calculated after 0.25 h of reaction, based on the total loading of metals. Reaction conditions: 50 °C, 10 mL, 0.3 M glycerol, NaOH: glycerol= 4, glycerol: M= 500, 3 bar O₂.

^e Calculated after 0.25 h of reaction, based on the total loading of metals. Reaction conditions: 50 °C, 10 mL, 0.3 M glycerol, NaOH: glycerol= 4, glycerol: M= 1000, 3 bar O₂.

^f Normalized for the surface atoms using the inverse of the surface average diameter. Reaction conditions: 60 °C, 10 mL, 0.3 M glycerol, NaOH: glycerol= 2, glycerol: Au= 50000 for Au/C and AuPd/C, glycerol: Pd= 3000 for Pd/C, 10 bar O₂.

^g TOF was calculated only when an exact NP size and clear surface composition were reported.

^h S₅₀ in parentheses represents the selectivity to glyceric acid at 50% glycerol conversion.

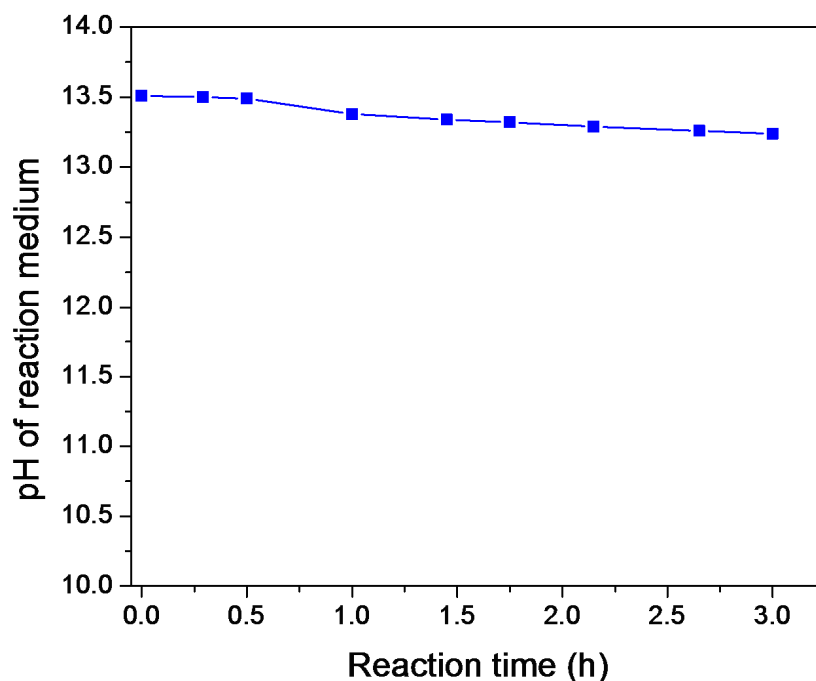


Figure S3. pH of reaction medium-time profile for glycerol oxidation reaction. Reaction conditions: 0.2 g 60 sc% Pd-on-Au/C, 60 °C, 1000 rpm, 107 mL, 0.1 M glycerol, 0.4 M NaOH, and 120 mL/min O₂ flow.

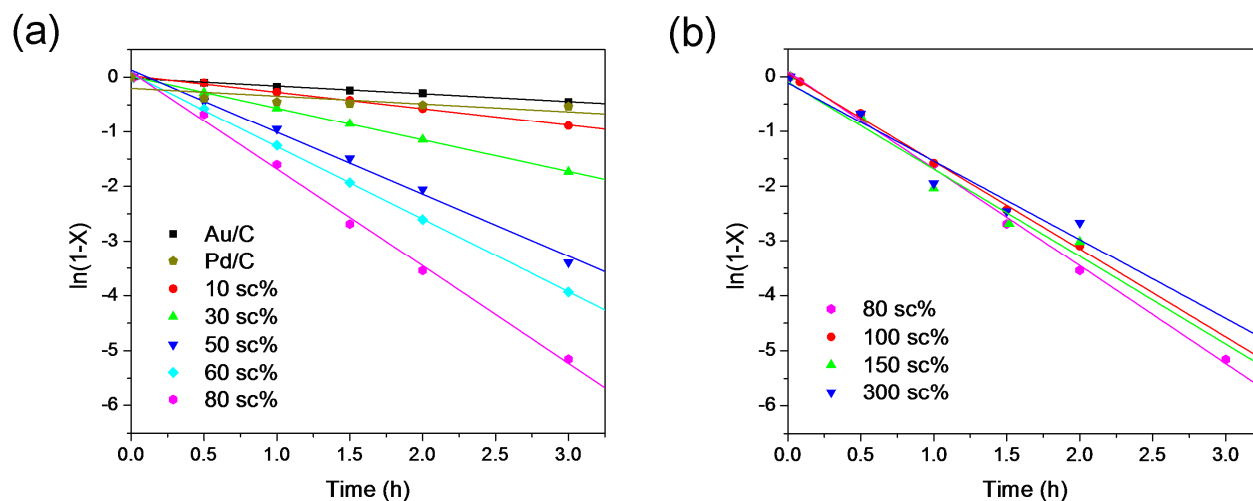


Figure S4. Plot of $\ln(1-x)$ vs. time for (a) Au/C, Pd/C, and 10 sc% to 80 sc% Pd-on-Au/C catalysts, (b) 80 sc% to 300 sc% Pd-on-Au/C catalysts. Solid lines are the fitted values to the first 2 hr of reaction profiles using 1st order kinetics for each catalyst.

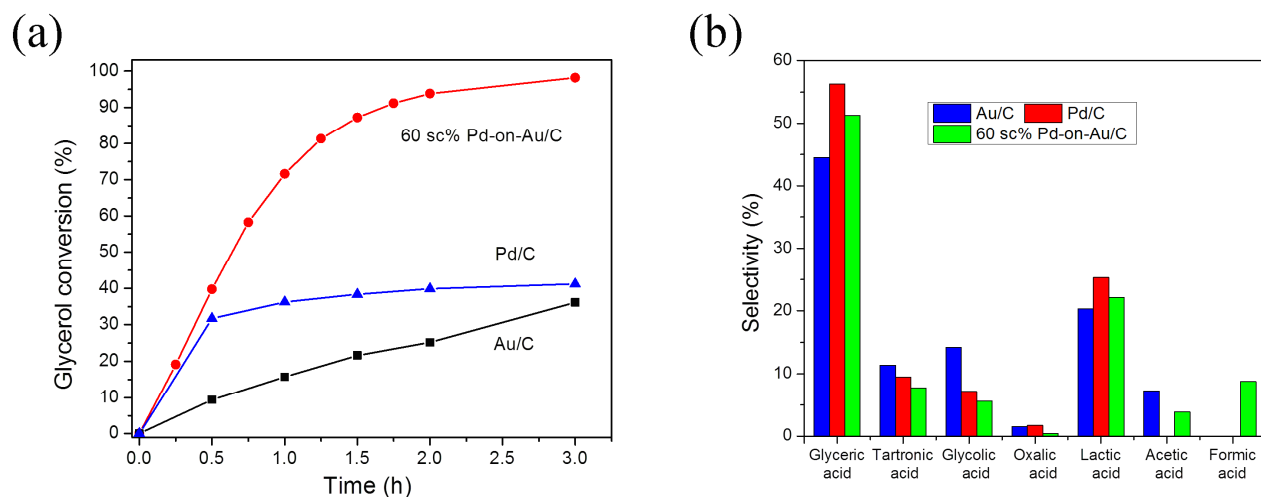


Figure S5. (a) Conversion-time profiles and (b) selectivity distributions at 30% glycerol conversion for Au/C, Pd/C and 60 sc% Pd-on-Au/C catalysts. Reaction conditions: 0.2 g catalyst, 60 °C, 1000 rpm, 107 mL, 0.1 M glycerol, 0.4 M NaOH, and 120 mL/min O₂ flow.

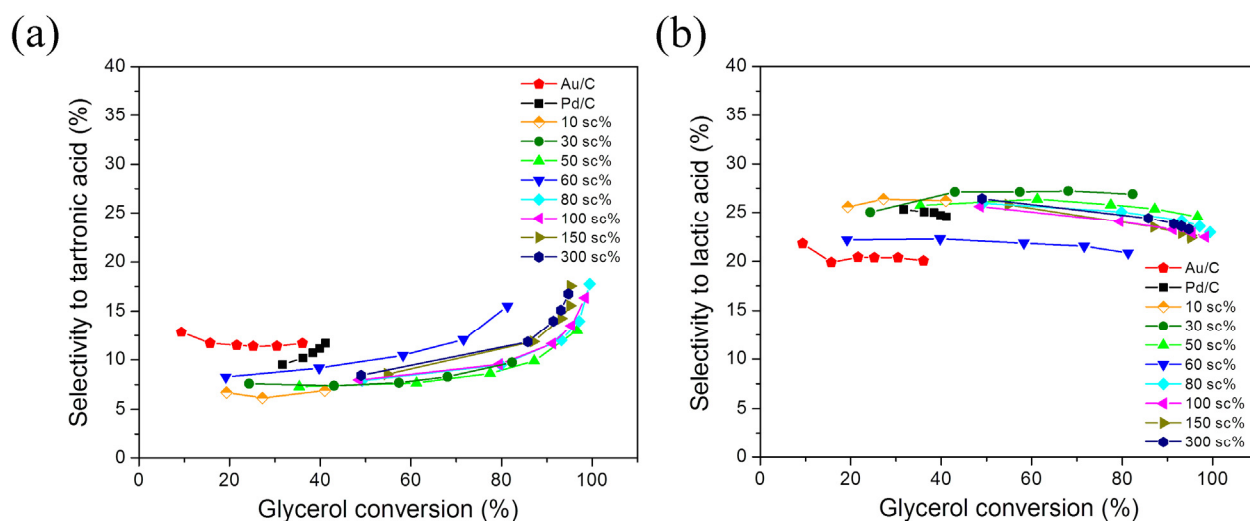
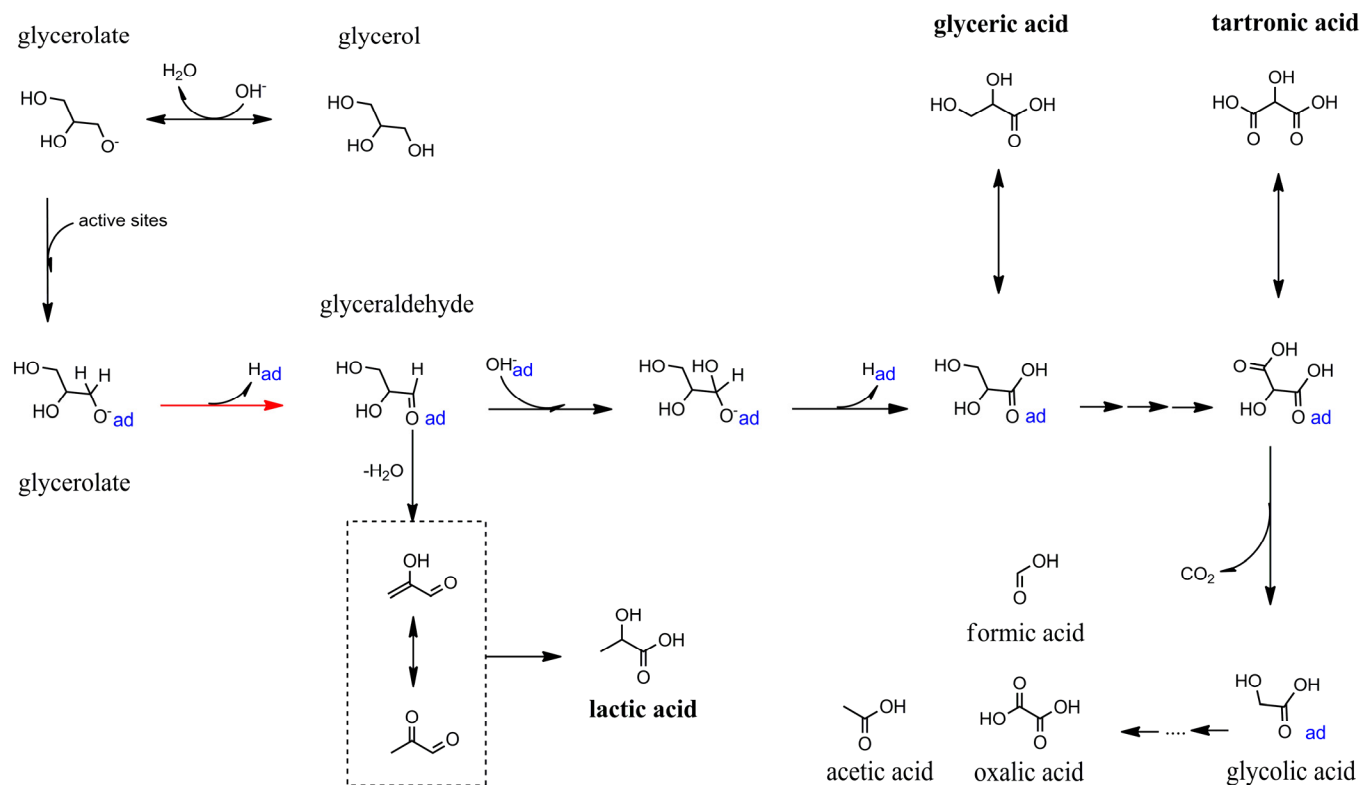


Figure S6. Plot of selectivity to (a) tartronic acid or (b) lactic acid vs. conversion of glycerol for Au/C, Pd/C, and Pd-on-Au/C catalysts. Reaction conditions: 0.2 g catalyst, 60 °C, 1000 rpm stirring rate, 107 mL, 0.1 M glycerol, 0.4 M NaOH, and 120 mL/min O₂ flow.

Table S2. Selectivity (normalized to all detected products) and carbon balance (sum of all carbons of detected C₁, C₂ and C₃ compounds divided by initial carbon content of glycerol) for Au/C, Pd/C and Pd-on-Au/C catalysts at 30% glycerol conversion.

Catalyst	Selectivity at 30% glycerol conversion (%)							Carbon balance at 30% glycerol conversion (%)
	Glyceric acid	Tartronic acid	Lactic acid	Glycolic acid	Oxalic acid	Acetic acid	Formic acid	
Au/C	45.3	11.4	20.3	14.2	1.5	7.3	0	93.3
10 sc%	44.5	6.3	26.4	7.8	0	2.8	12.2	93.2
30 sc%	47.5	7.5	25.7	6.1	0.1	3.0	10.1	91.5
50 sc%	46.5	7.2	25.6	5.8	0.4	4.5	10.0	92.4
60 sc%	51.3	7.8	22.1	5.6	0.4	3.9	8.8	91.3
80 sc%	48.9	6.9	26.5	5.4	0.4	3.3	8.5	92.0
100 sc%	51.6	7.0	26.6	5.4	0.5	1.2	7.8	91.2
150 sc%	52.9	6.0	27.6	5.9	0.5	0.6	6.5	90.5
300 sc%	50.2	6.7	27.5	7.9	0.9	0	7.6	89.9
Pd/C	56.3	9.5	25.3	7.2	1.7	0	0	81.0



Scheme S1. Proposed surface reaction of scission of glycerolate and scission of tartronate, and relation to detected species (major products in bold) using Au, Pd, and Pd-on-Au catalysts. Species in dashed boxes and surface intermediates (labeled "ad") were not detected and were inferred to be formed. The blue-colored subscript represents the surface activated species, and the red arrow shows the rate-limiting step of C-H bond cleavage at the beta carbon position to the secondary alcohol group. Reaction products are shown in their acid forms.

Table S3. List of apparent activation energies (E_a), and natural log of pre-exponential factors ($\ln(A)$) for Au/C, Pd/C, and 30 sc%, 60 sc%, 150 sc%, and 300 sc% Pd-on-Au/C catalysts.

Catalyst	E_a (kJ/mol)	$\ln(A)$
Au/C	45.4 ± 5.0	15.6 ± 3.1
Pd/C	50.6 ± 2.8	16.5 ± 0.8
30 sc%	40.0 ± 2.1	13.1 ± 0.9
60 sc%	38.7 ± 2.0	13.4 ± 1.0
150 sc%	39.5 ± 3.0	14.0 ± 0.5
300 sc%	40.9 ± 2.5	13.8 ± 0.8

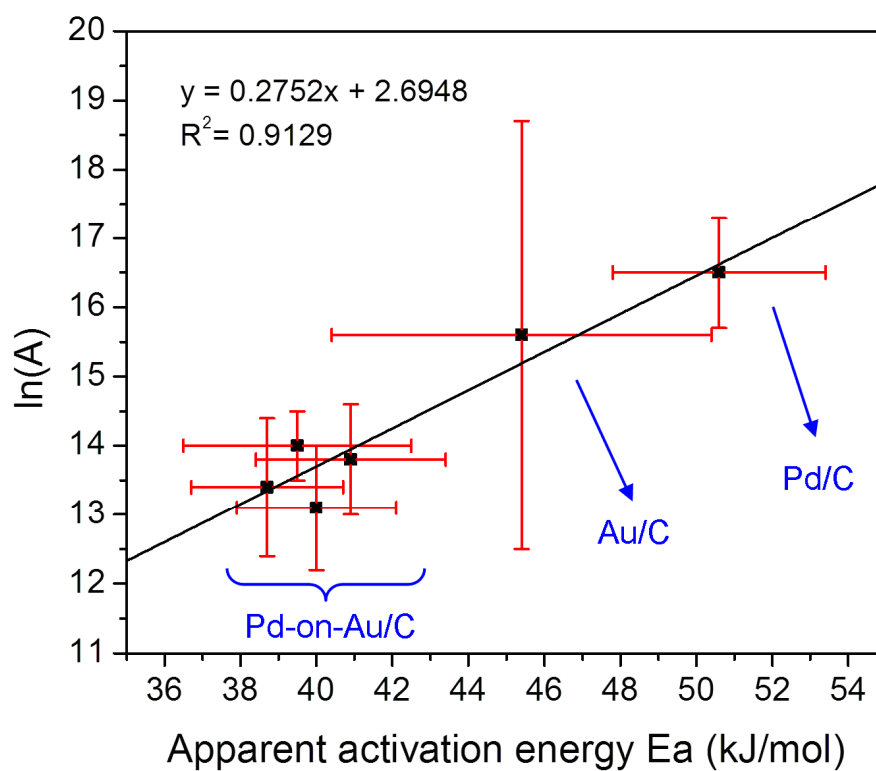


Figure S7. Plot of natural logarithm of pre-exponential factor $\ln(A)$ against apparent activation energy E_a .

Calculation of voltage potential E_h at reaction conditions:

The potential of water pE is associated with the redox couple: $O_2(g) + 4H^+ + 4e^- \rightarrow 2H_2O$. It can be calculated from: $pE = pE^0 + \log(P_{O_2}^{1/4}[H^+])$, where pE^0 is the standard potential at 333 K, P_{O_2} is the pressure of O_2 in atm and $[H^+]$ is the concentration of H^+ .¹³

Since $pE^0 \sim 1/T$, where T is temperature, $pE^0(333K) = pE^0(298K) \times 298/333 = 20.8 \times 298/333 = 18.6$. Then $pE = 18.6 + \log(10^{-13.5}) = 5.1$. The voltage potential of water is: $E_h = 0.0591 \times pE = 0.30$ V.

For the redox reaction: $Pd + H_2O \rightarrow PdO + 2H^+ + 2e^-$, the voltage potential of this reaction is expressed as: $E_h = E^0 - 2.303 \times RT/F \times pH$, where E^0 is the standard voltage potential at 298 K, R is the universal gas constant, T is temperature, and F is the Faraday constant.¹⁴ E^0 is dependent on temperature, and at elevated temperatures, E^0 is: $E^0(T) = E^0(298K) + (T - 298) \times (dE_0/dT)$.¹⁵ From literature, $E^0(298K) = 0.917$ V,^{16, 17} and $dE_0/dT = -0.45 \times 10^{-3}$ V/K.¹⁵ Thus, $E^0(333K) = 0.917 + (333-298) \times (-0.45 \times 10^{-3}) = 0.901$ V.

At 298K and $pH = 13.5$, $E_h = 0.901 - 2.303 \times RT/F \times pH = 0.10$ V. At 333K (glycerol oxidation reaction temperature) and $pH = 13.5$ (reaction pH), $E_h = 0.901 - 2.303 \times RT/F \times pH = +0.01$ V.

References

1. J. M. Thomas, *Pure and Applied Chemistry*, 1988, **60**, 1517-1528.
2. L. Lewis, *Chemical Reviews*, 1993, **93**, 2692-2730.
3. T. Teranishi and M. Miyake, *Chemistry of Materials*, 1998, **10**, 594-600.
4. M. O. Nutt, K. N. Heck, P. J. J. Alvarez and M. S. Wong, *Applied Catalysis B: Environmental*, 2006, **69**, 115-125.
5. Y. L. Fang, K. N. Heck, P. J. J. Alvarez and M. S. Wong, *ACS Catalysis*, 2011, **1**, 128-138.
6. G. D'Errico, O. Ortona, F. Capuano and V. Vitagliano, *Journal of Chemical & Engineering Data*, 2004, **49**, 1665-1670.
7. S. Demirel, M. Lucas, J. Warna, D. Murzin and P. Claus, *Top Catal*, 2007, **44**, 299-305.
8. N. Dimitratos, F. Porta and L. Prati, *Applied Catalysis A: General*, 2005, **291**, 210-214.
9. N. Dimitratos, J. A. Lopez-Sanchez, J. M. Anthonykutty, G. Brett, A. F. Carley, R. C. Tiruvalam, A. A. Herzing, C. J. Kiely, D. W. Knight and G. J. Hutchings, *Physical Chemistry Chemical Physics*, 2009, **11**, 4952-4961.
10. C. Bianchi, P. Canton, N. Dimitratos, F. Porta and L. Prati, *Catalysis Today*, 2005, **102-103**, 203-212.
11. A. Villa, C. Campione and L. Prati, *Catalysis Letters*, 2007, **115**, 133-136.
12. W. Ketchie, M. Murayama and R. Davis, *Journal of Catalysis*, 2007, **250**, 264-273.
13. W. Stumm and J. J. Morgan, *Aquatic Chemistry: Chemical Equilibria and Rates in Natural Waters, 3rd Edition*, Wiley, 1995.
14. E. McCafferty, *Introduction to Corrosion Science*, Springer, 2010.
15. S. G. Bratsch, *Journal of Physical and Chemical Reference Data*, 1989, **18**, 21.
16. M. Pourbaix, *Atlas of Electrochemical Equilibria at 25 °C*, Gauthier-Villars, Paris, 1963.
17. A. J. Bard, R. Parsons and J. Jordan, *Standard Potentials in Aqueous Solution*, CRC Press, 1985.